On the Characteristics of Gravity Waves Generated by Atmospheric Shear Layers

D. P. LALAS

Department of Mechanical Engineering Sciences, Wayne State University, Detroit, Mich. 48202

F. EINAUDI

Cooperative Institute for Research in Environmental Sciences, University of Colorado/NOAA, Boulder 80309 and Aeronomy Laboratory, NOAA, Boulder, Colo. 80302

(Manuscript received 20 November 1975, in revised form 9 March 1976)

ABSTRACT

The stability analysis of a hyperbolic tangent velocity profile in an isothermal atmosphere in the presence of the ground is presented. It is shown that such a system has a number of modes in addition to the one studied by Drazin and that unstable waves can be excited, for finite values of some minimum Richardson number of the flow, even in the limit of horizontal wavelengths going to infinity. Some of the unstable waves belonging to these new modes are able to propagate energy and momentum away from the shear zone and may therefore play an important role in microscale flow dynamics and in coupling of small-scale phenomena to mesoscale flow motions.

1. Introduction

The excitation of gravity waves by shear flow instability has been extensively investigated in order to explain a variety of phenomena in the ocean and the atmosphere. We will focus here on only some of the pertinent results. The interested reader is referred to the review articles of Drazin and Howard (1966), Thorpe (1973) and Howard and Maslowe (1973) for more complete and detailed discussion of previous work. Of the wind profiles utilized to model a shear layer, the simplest is the Helmholtz profile, which has a background horizontal velocity $U_0(z)$ constant in each of two semi-infinite media and a sharp discontinuity at the separating interface. Recently, some new properties of this profile have been reported by Lindzen (1974), and also by Einaudi and Lalas (1974) who, in addition, take into account temperature discontinuities and condensation effects. Other models utilized are, in order of increasing correspondence to reality and difficulty, a constant shear layer between constant velocity layers (Taylor, 1931; Goldstein, 1931; Miles and Howard, 1964; Jones, 1968; Gossard, 1974), and a $U_0(z)$ given by a hyperbolic tangent (Drazin, 1958; Maslowe and Kelly, 1971; Thorpe, 1973). The stability investigations of the above profiles are complemented by the general stability results of Miles (1961), Howard (1961) and Chimonas (1970) that provide bounds on the range of the phase velocities and growth rates of the unstable waves through the so-called semicircle theorem, as well as a sufficient condition for stability.

The primary aim of these investigations is to specify, for given velocity and density or temperature profiles, the characteristics of the most unstable wave to be excited, i.e., its wavelength, period, phase velocity and growth rate, as well as the range of horizontal wavelengths λ_x that are unstable for a given value of some characteristic Richardson number of the flow. Thus, Drazin (1958), investigating a hyperbolic tangent velocity profile with an exponentially decreasing density in an infinite medium, finds that the neutral stability boundary is given by $J=\alpha^2(1-\alpha^2)$, where J is the minimum Richardson number in the flow and α the product of the horizontal wavenumber $k_x=2\pi/\lambda_x$ of the disturbance and half the depth of the shear layer. The most unstable wave corresponds to $J=0$ and $\alpha\approx 0.44$ (Maslowe and Kelly, 1971). For the Miles and Howard (1964) model, of a constant shear layer with linearly decreasing density between two semi-infinite layers of uniform velocity and density, the most unstable wave is associated with $J=0$ and $\alpha\approx 0.41$. Both results have been used extensively in analyzing experimental observations in the atmosphere (Atlas *et al.*, 1970; Emmanuel, 1973; Hooke *et al.*, 1973) and the ocean (Woods, 1968).

A common property of Drazin's and Miles and Howard's models is the existence of one mode only, for which the instability domain in the (α,J) plane is bounded by its singular neutral mode; furthermore, unstable waves with $\alpha\rightarrow 0$ require correspondingly small values of the Richardson number, which are un-

common in the atmosphere. Because of such properties, the above two models may not be able to explain satisfactorily some recent observations obtained by improved remote sensing techniques such as FM-CW radars, acoustic sounders, Doppler radars, etc., together with microbarograph arrays and instrumented high meteorological towers. In particular, the appearance on a number of occasions (Reed and Hardy, 1972; Hooke and Hardy, 1975) of more than one wave with different horizontal wavelengths and the detection of gravity waves with horizontal wavelengths of the order of 100–500 km (Uccellini, 1975; Lilly, private communication) may require, in our opinion, the existence of a modal structure associated with a given velocity and temperature profile, with at least one mode associated with very large wavelengths.[1]

Jones (1968) indeed finds a modal structure in one of the three profiles he considers. He examines numerically three models of a constant shear layer capped by a semi-infinite layer of constant velocity, with a background density which decreases exponentially with height; adjacent to the bottom of the shear layer in the first case is the ground, in the second case another finite layer of constant velocity and then the ground, and in the third a semi-infinite layer of constant velocity with no ground at all. Jones finds that the first model is always stable, the second unstable for all wavenumbers, and the third unstable for wavenumbers larger than some wavenumber k_0. In the second model, he finds one mode only whose singular neutral curve has two branches, one of which corresponds to propagating waves in the top layer. In the third model, he finds two singular neutral modes, bounding two areas of instability that overlap for a finite range of wavenumbers $k_1 \geqslant k_x \geqslant k_0$ within which one mode is evanescent in the upper semi-infinite layer and the other in the lower. For $k_x > k_1$ only one mode exists and is evanescent in both top and bottom layers. More recently, Dickinson and Clare (1973) and Dickinson (1973) have analyzed numerically an unbounded hyperbolic-tangent barotropic shear flow, and the corresponding baroclinic shear problem, respectively. In both studies, two modes exist for sufficiently small values of the longitudinal wavenumbers, one of which is propagating. Finally, very recently, Blumen *et al.* (1975) have found a second unstable mode, which exists only when the Mach number is greater than 1, in a hyperbolic-tangent shear layer profile in the absence of gravity and stratification. This new mode decays away from the shear zone much more slowly than the subsonic one.

The fact that unstable modes are present in the limit $k_x \to 0$, in Jones' second model, while no unstable mode exists for $k_x < k_0$ when the ground is removed, suggests that the presence of the ground may destabilize the longer horizontal wavelengths. This is confirmed by the results of Hazel (1972), who investigates numerically a class of shear flows with different velocity and density profiles, bounded on top and bottom by solid surfaces. His results clearly indicate that the presence of solid boundaries destabilizes the long wavelengths and stabilize the short wavelengths at a smaller rate. When, on the other hand, the boundaries are brought too close to each other, the system becomes completely stable in accordance with Howard's (1964) calculations. Similar results are obtained by Einaudi and Lalas (1976) who considered the stability of Drazin's profile in the presence of two solid boundaries. In addition to the mode that would correspond to Drazin's if the boundaries were removed, they find a number of new modes, all of which are unstable, for finite values of J, as $\alpha \to 0$. The presence of a solid top boundary is unrealistic for atmospheric applications, at least as far as the propagating modes are concerned, because it does not allow leakage of energy away from the shear layer. To rectify this shortcoming, Lalas *et al.* (1976) have investigated the characteristics of a Helmholtz profile with a solid lower boundary at a finite distance below the velocity discontinuity. Contrary to the results without the ground (Einaudi and Lalas, 1974), they find that an infinite number of unstable modes exists even for horizontal wavelengths of the order of tens of kilometers with the most unstable new modes in reasonable agreement with experimental observations.

In an attempt to determine all possible modes of an atmospheric shear flow configuration that is more realistic than a Helmholtz profile, or a constant shear profile, we examine in this paper the inviscid stability of a semi-infinite hyperbolic-tangent horizontal background flow along the x direction, i.e.,

$$U_0(z) = V \tanh(z/h), \tag{1}$$

with the origin of the coordinate system (x,z) at the height of the inflexion point and the ground some finite distance $|z_i|$ below. The effective width of the shear layer obeying (1) is given by $2h$. We also assume the atmosphere to have a background density ρ_0 given by

$$\rho_0(z) = \rho_g \exp(-z/H), \tag{2}$$

where H is the scale height of the atmosphere and ρ_g the density at the inflexion height. A density of the form given by Eq. (2) implies a constant Brunt–Väisälä frequency n and a constant background temperature $T_0 = g/RH$, where g is the gravitational acceleration acting in the negative z direction and R is the gas constant for air. The velocity U_0 and density ρ_0 are shown, not in scale, in Fig. 1.

The mode previously discussed by Drazin is recovered, but with some significant differences in the values of the frequency at large wavelengths. Furthermore, additional modes are shown to exist with most

[1] For convenience, we will, in this paper, refer to unstable waves that end on different neutral curves in the normalized (α, J) plane as belonging to different modes, even though in a different projection of the stability boundary, one mode may simply be the continuation of another.

unstable wavelengths, for the same J, that are two or three times longer than the most unstable one of the main mode. Unstable waves can be excited at finite J, even in the limit of $\alpha \to 0$. Some of these additional modes are predominantly propagating, rather than evanescent, at large heights where there is no shear. Growth rates and stability boundaries for these modes are calculated, and the effect of the distance of the shear layer to the ground is discussed. Finally, the effect of a sudden increase in stability at large distances from the ground, as is often the case at the tropopause, is explored briefly.

2. The governing equations

As previously mentioned, we assume a stratified shear flow in the atmosphere with a hyperbolic-tangent wind profile and constant Brunt–Väisälä frequency, bounded below by a solid surface, the ground, and above by an infinite layer with constant wind and temperature, as shown in Fig. 1. We are interested in investigating the characteristics of unstable and neutral gravity waves that can be supported in such an atmosphere. If this background flow is perturbed by disturbances that are small enough so that they are adequately described by the linearized version of the inviscid hydrodynamic equations, and if use is made of the Boussinesq approximation, the equations of conservation of mass, horizontal momentum and vertical momentum, and the condition of incompressibility take the form

$$\frac{\partial u_1}{\partial x}+\frac{\partial w_1}{\partial z}=0 \tag{3}$$

$$\rho_0\left(\frac{\partial}{\partial t}+U_0\frac{\partial}{\partial x}\right)u_1+\rho_0\frac{dU_0}{dz}w_1+\frac{\partial p_1}{\partial x}=0 \tag{4}$$

$$\rho_0\left(\frac{\partial}{\partial t}+U_0\frac{\partial}{\partial x}\right)w_1+\frac{\partial p_1}{\partial z}+g\rho_1=0 \tag{5}$$

$$\left(\frac{\partial}{\partial t}+U_0\frac{\partial}{\partial x}\right)\rho_1-\frac{n^2}{g}\rho_0 w_1=0. \tag{6}$$

In Eqs. (3)–(6), u_1, w_1, p_1 and ρ_1 denote the horizontal velocity, vertical velocity, pressure and density, respectively, of the disturbance; U_0 and ρ_0 are defined by (1) and (2), respectively; and n^2 is given by

$$n^2=-g\left(\frac{1}{\rho_0}\frac{d\rho_0}{dz}+\frac{g}{c_0^2}\right)=g\frac{d\theta_0}{dz}\Big/\theta_0, \tag{7}$$

where c_0 is the speed of sound and θ_0 the potential temperature. To be consistent with the Boussinesq approximation utilized in (3)–(6) the term g/c_0^2 in (7) should be omitted. This point and the validity of the Boussinesq approximation will be discussed later. In this investigation, since we are not interested in convectively unstable flows n^2 is taken to be real and positive.

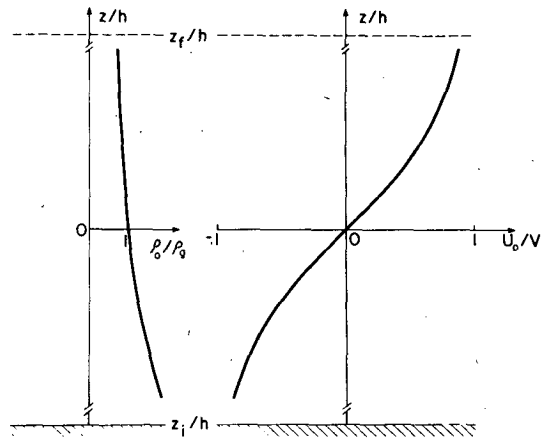

FIG. 1. The normalized density and velocity profiles and the geometry of the basic flow (not in scale).

For a disturbance of wavelength λ_x, wavenumber $k_x=(2\pi/\lambda_x)$ and complex frequency $\omega=\omega_r+i\omega_i(\omega_i>0)$, we assume a perturbation vertical velocity w_1 of the form

$$w_1=\rho_0^{-\frac{1}{2}}\,\mathrm{Re}\{\psi(z)\exp[i(k_x x-\omega t)]\}. \tag{8}$$

Eliminating u_1, p_1 and ρ_1, also assumed to possess similar forms, in favor of w_1 in (3)–(6), we obtain the following equation for ψ:

$$\frac{d^2\psi}{dy^2}-\Lambda(y)\psi=0, \tag{9}$$

with

$$\Lambda=\left[\alpha^2+\frac{\sigma^2}{4}-\frac{J}{\Omega^2}-\left(\frac{d^2u_0}{dy^2}-\sigma\frac{du_0}{dy}\right)\Omega^{-1}\right]. \tag{10}$$

The normalized quantities that appear in Eq. (10) are defined as follows:

$y=z/h$	normalized height coordinate
$\alpha=hk_x$	normalized horizontal wavenumber
$c_r=\omega_r/k_xV$	normalized horizontal phase velocity of the wave
$c_{re}=c_r-u_0$	normalized Doppler-shifted phase velocity
$c_i=\omega_i/k_xV$	normalized imaginary part of the frequency of oscillation
$\Omega=c_{re}+ic_i$	normalized Doppler frequency
$\sigma=h/H$	ratio of the scale length of velocity to that of density
$u_0(y)=U_0/V=\tanh y$	normalized background velocity
$J=n^2h^2/V^2$	value of the Richardson number at $y=0$; also the minimum Richardson number of the flow domain.

In the present notation, the local Richardson number

Ri becomes

$$\mathrm{Ri}=J\left(\frac{du_0}{dy}\right)^{-2}, \tag{11}$$

so that $\mathrm{Ri}>J$ everywhere in the flow domain except at $y=0$, the inflexion point, where $\mathrm{Ri}=J$.

Even though the Boussinesq approximation has been utilized, it should be pointed out that the effect of the background density variation in the inertial term of the momentum equation is included in (9) and gives rise to the terms, proportional to σ, which we shall henceforth call inertial terms of the density gradient.

The boundary or radiation conditions to be imposed on ψ are as follows:

(i) At $y=y_i=z_i/h$, where z_i is the distance of the ground from the inflexion point,

$$\psi(y_i)=0. \tag{12}$$

(ii) Above some height $y_f=z_f/h$, u_0 is virtually constant and so is $\Lambda(y)$. In this region, the solution takes the form $\psi\sim\exp(iKy)$ [see Hines, 1974], where K is the normalized vertical wavenumber given by

$$K=\pm[-\Lambda(y=y_f)]^{\frac{1}{2}}=K_r+iK_i. \tag{13}$$

The perturbation amplitude has to go to zero at $y=\infty$ or, if the wave is neutral and propagating, it has to obey the usual radiation condition. This is assured if the sign in (13) is chosen so that either $K_i>0$ or, when $K_i=0$, $dc_r/dK_r>0$. For a wave of the form $\psi\propto\exp(iKy)$, the following relation has to hold between ψ and $d\psi/dy$:

$$\frac{d\psi}{dy}=iK\psi \quad \text{at} \quad y=y_f. \tag{14}$$

It may be noted that for all values of $y>5$, du_0/dy is essentially zero and (14) holds for all $y_f\geqslant 5$.

All unstable waves of given horizontal wavelength that can be supported by a stratified shear, described by Eqs. (1) and (2) and characterized by a given J and α, will have frequency c_r and growth rate αc_i given by the eigenvalue problem for c_r and c_i comprising Eq. (9) and boundary conditions (12) and (14). Similarly, singular neutral waves that exist in a flow characterized by some J will have frequency c_r and wavenumber α given by the same eigenvalue problem with $c_i=0$ in (9), (12) and (14). The fact that now $c_i=0$ introduces possible singularities in (9) and the numerical difficulties that result and their resolutions will be discussed in the next section.

3. Numerical procedure

A stability analysis of a fluid flow should be able to provide the main characteristics of unstable modes such as frequency, phase velocity and growth rate in terms of the parameters of the basic flow, i.e., in terms of z_i, n^2, V and h. In addition, it should provide stability boundaries in the (α,J) plane that can specify the range of unstable wavelengths λ_x for a given physical situation. The domain of unstable modes will be bounded by contiguous neutral modes. Since according to the semicircle theorem (Miles, 1961; Howard, 1961) the horizontal phase velocity of unstable modes has to be equal to the background velocity at some height y_c, known as the critical level, contiguous neutral modes will possess a critical level as well, where now (9) becomes singular. The altered nature of (9) when $c_i=0$ necessitates the use of one program for unstable waves and another for singular neutral modes. For both, the integrating subroutine utilized is the one developed by Bulirsch and Stoer (1966). A comparison of its performance versus other standard techniques, like the Runge–Kutta, can be found in Hull *et al.* (1972). The details of the two programs follow.

a. Program for the unstable modes

To determine the appropriate c_r and c_i for given α and J, some trial values of c_r and c_i are assumed and Eq. (9) is then integrated from $y=y_i$ to $y=y_f$. If the resulting values of ψ and its derivative at $y=y_f$ satisfy (14), the trial values of c_r and c_i are accepted as the true ones. Otherwise new values for c_r and c_i are assumed and the procedure is repeated until (14) is satisfied. No difficulty is encountered in obtaining the correct c_r and c_i, after a few iterations, for the entire range of α and J. All eigenvalues are correct to at least four significant figures.

b. Program for the singular neutral modes

In this case, for given α, values for c_r and J are assumed and Eq. (9) is integrated starting simultaneously at both $y=y_i$ and $y=y_f$ to within a small distance y_m away from the critical level y_c, i.e., up to $y=y_c-y_m$ and down to $y=y_c+y_m$, respectively, where $0<y_m\ll 1$.

The analytical Frobenius expansion of ψ (Ince, 1956), valid in $y_c-y_m\leqslant y\leqslant y_c+y_m$, is used to match the numerically calculated ψ at both sides of the critical level, if the assumed c_r and J are indeed eigenvalues. If the matching is not possible, new values of c_r and J are assumed, as before, and the entire procedure is repeated until the matching is obtained.

The difference between this program and Hazel's (1972) second program discussed in his Appendix A, apart from the integrating routine, is the ability of our program to investigate neutral modes of arbitrary phase velocity and unknown position of the critical level.

The values of c_r and hence y_c are found to be sensitive to the value of y_m. If y_m is too large, a large number of terms in the Frobenius expansion is necessary, and in some cases up to three terms are utilized. If y_m is too small, numerical difficulties arise because of the large values of the derivatives near y_c. Usually, a value of

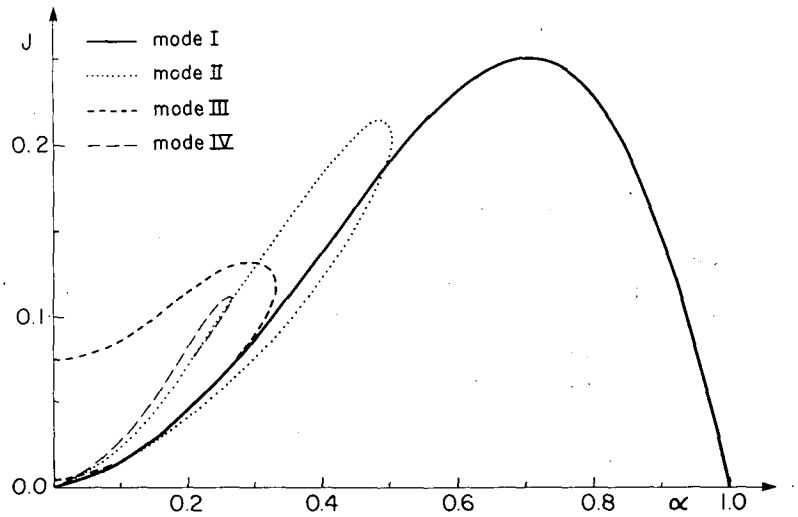

FIG. 2. Stability boundaries, in the normalized wavenumber, minimum Richardson number (α,J) plane for modes I, II, III and IV for $y_i=-10$, $y_f=10$, $\sigma=0.1$. Note that the lower branches of modes II and III overlap in part with mode I and the lower branch of mode IV with the upper branch of mode II.

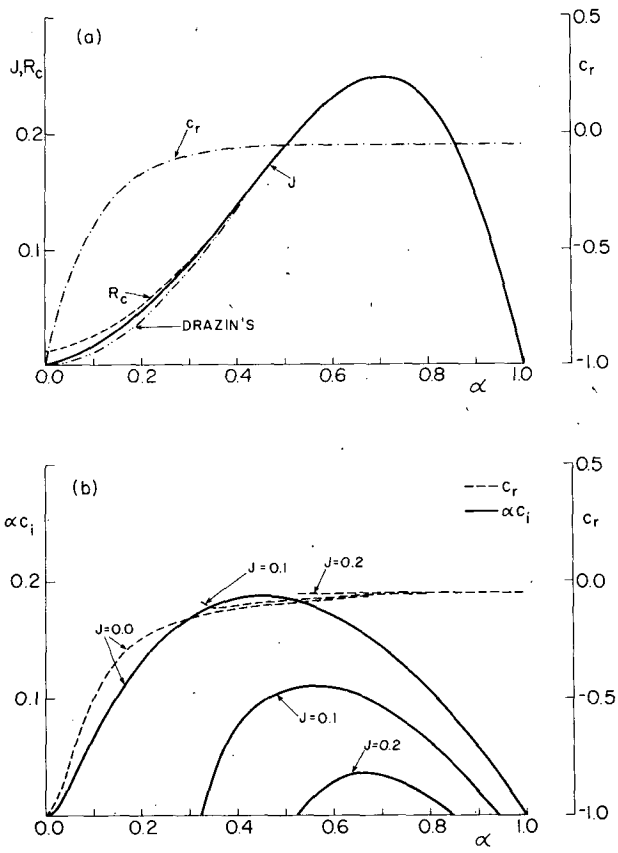

FIG. 3. Mode I stability characteristics for $y_i=z_i/h=-10.0$, $y_f=z_f/h=10.0$ and $\sigma=0.1$. (a) J (solid line), R_c (dashed line) and corresponding c_r (dot-dashed line) as a function of $\alpha=k_xh$ for the neutral waves. The dash-double dotted line labeled "Drazin's" corresponds to $\sigma=0.0$ and $y_i\to-\infty$, $y_f\to\infty$; (b) normalized growth rates αc_i (solid lines) and phase velocities c_r (dashed lines) as a function of α for different values of J for the unstable waves.

$y_m=10^{-4}$ and a one-term series expansion are found to be adequate.

The agreement between the two programs is excellent and, as can be seen from the figures, unstable modes end exactly on neutral modes in the (α,J) plane, except for those modes which intersect the $\alpha=0$ axis and thus do not end on a neutral curve.

4. Results

The number of the parameters specifying the background flow, i.e., n^2, h, V, J, z_i, etc., is so large that one is forced to limit the investigation to specific parametric studies, three of which are presented below.

a. Results for constant shear thickness 2h

The neutral curves and the properties of the unstable waves are calculated for three different locations of the shear layer inflexion point with respect to the ground. Specifically, the normalized distance between the ground and the inflexion point $y_i=z_i/h$ is taken to be -10.0, -5.0 and -2.0. The normalized height, $y_f=z_f/h$, above which we consider the velocity to be uniform and at which we take (14) to hold, is taken to be 10.0, although any value larger than 5.0 is adequate and no appreciable effect on the eigenvalues and the eigenfunctions is noted. The ratio σ of half the shear layer thickness h to the density scale height H is taken to be $\sigma=h/H=0.1$; calculations with $\sigma=0$ are also carried out to ascertain the effect of inertial terms of the density gradient.

Following Thorpe (1969), we choose J as the main stability parameter. For given J, once the phase velocity of a particular mode is known, the value of R_c, the

Richardson number at the critical level for that wave, where $u_0=c_r$, can be calculated from the relation

$$R_c=\mathrm{Ri}(y_c)=J/(1-c_r^2)^2. \quad (15)$$

For each particular geometry we calculate the characteristics of both unstable and neutral modes that may be excited. For the unstable modes, normalized growth rates $\alpha c_i=\omega_i h/V$ and phase velocities c_r are plotted versus $\alpha=k_x h$, for selected values of J. For the neutral modes, c_r, J and R_c are plotted versus α.

For $z_i/h=-10.0$, at least four modes, which we shall call modes I, II, III and IV in order of decreasing growth rates, are found. The neutral curves that comprise the stability boundary for each mode are shown in Fig. 2. The properties of the first three modes are shown in more detail in Figs. 3 and 4. The additional modes IV, V, etc., have growth rates too small to plot and in addition the range of α over which they exist is very narrow. We shall therefore ignore them in the following discussion. For relatively large values of α, only mode I is allowed, with c_r of the order of -0.05. If $\sigma=0$, the growth rates and the neutral curve for mode I remain the same to less than 1% but c_r is now zero for large α. As $z_i\to-\infty$, mode I coincides with the one found by Drazin (1958) and shown for comparison in Fig. 3a. Modes I and II correspond to waves that are mostly evanescent at large y, i.e., $K_i\gg|K_r|$ with K defined in (13), while mode III corresponds to mostly propagating waves, i.e., $|K_r|\gg K_i$. Near the ground, on the other hand, mode II is mostly propagating, mode I is mostly evanescent, while mode III can be either, depending on the particular values of α and J.

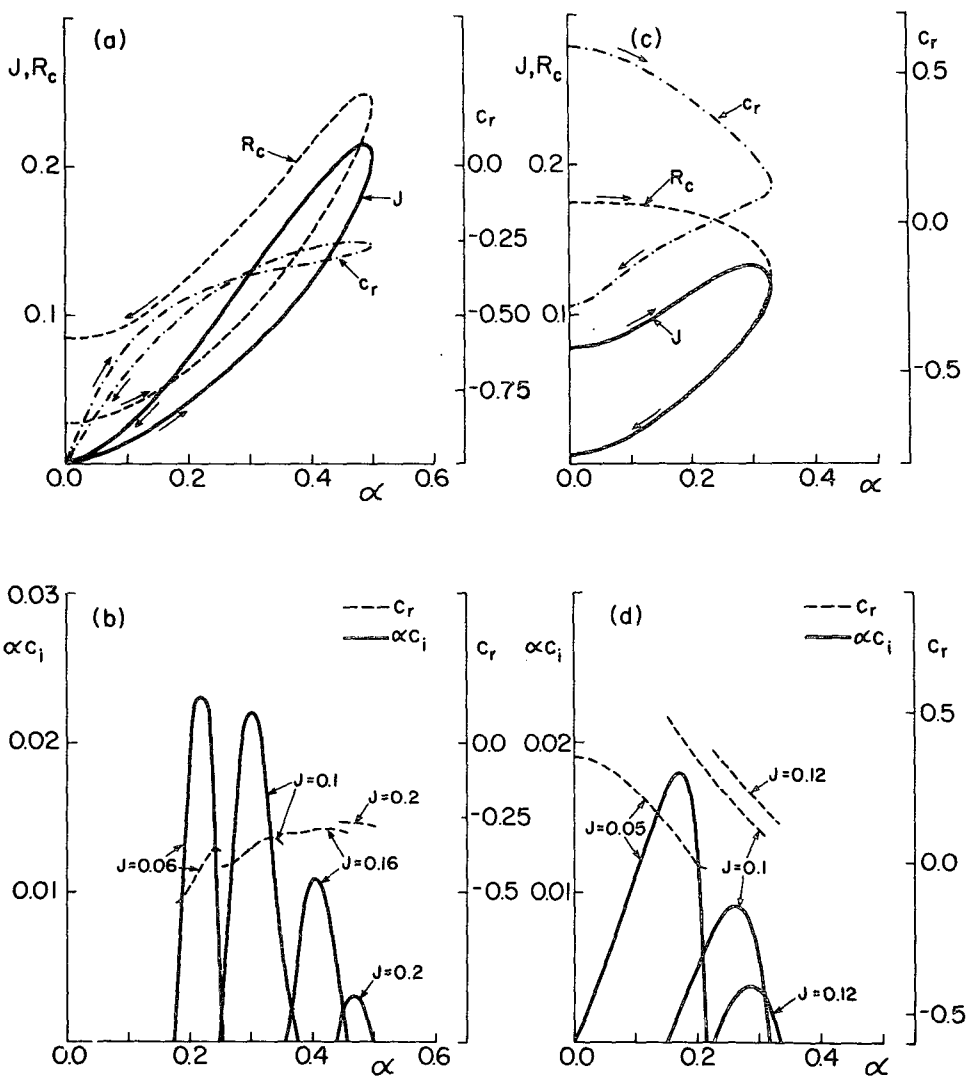

FIG. 4. Mode II and III characteristics for $y_i=-10.0$ and $y_f=10.0$ and $\sigma=0.1$ as in Fig. 3: (a) J (solid), R_c (dashed) and c_r (dot-dashed) vs α for mode II neutral waves; (b) αc_i (solid) and c_r (dashed) vs α for different J of mode II unstable waves; (c) as in (a) but for mode III; (d) as in (b) but for mode III.

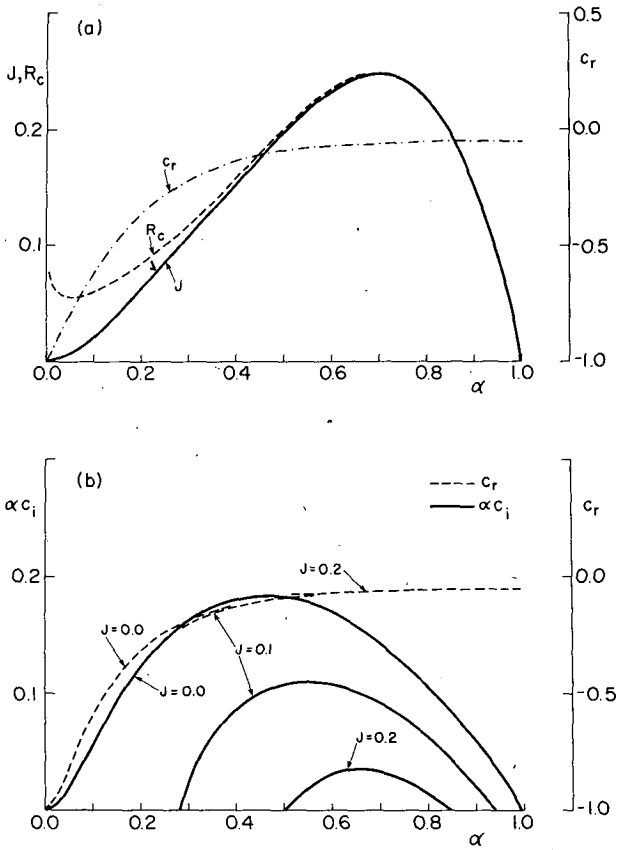

FIG. 5. As in Fig. 3 except for $y_i=z_i/h=-5.0$, mode I.

Figs. 5 and 6 show the wave characteristics for the case of $z_i/h=-5.0$. In this case, mode II has disappeared. The growth rates of mode III are larger than the ones for $z_i/h=-10.0$. Finally, for $z_i/h=-2.0$, the results are plotted in Fig. 7. Mode III has now disappeared as well. The maximum value of α for unstable modes to exist has decreased to $\alpha\approx 0.96$; if $|z_i/h|$ is decreased even further, this maximum value of α will decrease more and eventually even mode I will disappear in agreement with the results of Jones (1968, first model).

The effect of the distance from the inflexion point to the ground for the propagating mode can be seen more clearly in Fig. 8 where c_i of mode III for $\alpha=0.01$ is plotted versus z_i/h, for different values of J.

For mode I, at $J=0.0$, the most unstable wavelength corresponds approximately to $\alpha_{\max}\approx 0.46$. The value of α_{max} changes somewhat as J varies between 0 and 0.25; the growth rate αc_i undergoes much larger relative changes as J varies and reaches its maximum at $J=0.0$, as can be seen from Figs. 3b, 5b and 7b. For modes II and III the most unstable wavelength for given J is a much stronger function of J than for mode I as can be seen from Figs. 4b, 4d and 6b; for example, in Fig. 4d for mode III, at $J=0.1$, $\alpha_{\max}\approx 0.25$ while at $J=0.05$, $\alpha_{max}\approx 0.15$. The loci of the most unstable wavelengths for each J of modes II and III are lines running almost parallel to the neutral curves that comprise the lower neutral boundary (i.e., bottom solid lines in Figs. 4a, 4c and 6a). Again the actual growth rate αc_i changes as J changes. The approximate values of α and J at which the growth rate αc_i is maximum over the entire (α,J) plane, are given in Table 1, for each mode and for each of the three values of z_i/h considered.

The phase velocity of all modes that are mostly evanescent on top (i.e., I, II, IV, etc.) is seen to go to -1 for long wavelengths, with corresponding critical levels going toward the lower edge of the shear layer, where the local Richardson number is large; thus the growth rates will be small.

The eigenfunctions $Z_c=\mathrm{Re}(\psi)$ and $Z_s=-\mathrm{Im}(\psi)$ that correspond to the most unstable wavelengths of each mode for $z_i/h=-10.0$ and $J=0.1$ are plotted in Fig. 9. The normalization is with respect to the value of their

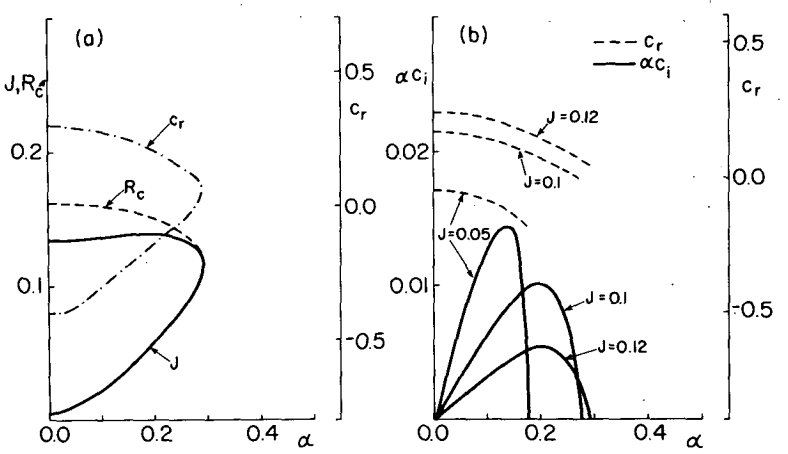

FIG. 6. As in Figs. 4c and 4d except for $y_i=-5.0$, mode III.

derivatives on the ground so that

$$\left(\frac{dZ_c}{dy}\right)_{y_i} = \left(\frac{dZ_s}{dy}\right)_{y_i} = 1.0. \tag{16}$$

This normalization scheme is chosen with the idea that microbarograph data on the ground can be used to provide the amplitude for specific cases. In Fig. 10, the eigenfunctions of mode I for $J=0.0$ and $\alpha=0.01$ are plotted for $z_i/h=-10.0$ and $z_i/h=-2.0$ to demonstrate the effects of the distance of the ground from the inflexion point.

Additional information concerning the modes described in Fig. 9 is given in Table 2, where the normalized vertical wavelength $\lambda_z=2\pi/K_r$ and the normalized vertical e-folding length $\delta_z=1/K_i$ are expressed in terms of the distance $\Delta y=|(y_i-y_c)|$ between the critical level and the ground. The values of λ_z and δ_z are calculated at $y=y_f$ and $y=y_i$, i.e., well in the regions of almost constant velocity. As can also be seen from Fig. 9, mode I is mostly evanescent above and below while mode II is mostly evanescent above but propagating below. Mode III is mostly propagating above; in the lower region it is propagating but K_i and K_r are of the same order. Furthermore, in the bottom layer and for $J=0.1$, mode II has a λ_z which is approximately twice Δy and mode IV (which is not shown in Fig. 9 but which has similar characteristics to those of mode II) has a horizontal phase velocity which is about twice that of mode II and a $\lambda_z/\Delta y$ of about 1. It appears therefore that the modes which are mostly propagating in the bottom layer may be due to resonance between the critical level and the solid surface below, as suggested by Lilly (private communication) and in qualitative agreement with the "quantization of the real part of the vertical wavenumber" observed by Lindzen and Rosenthal (1976).

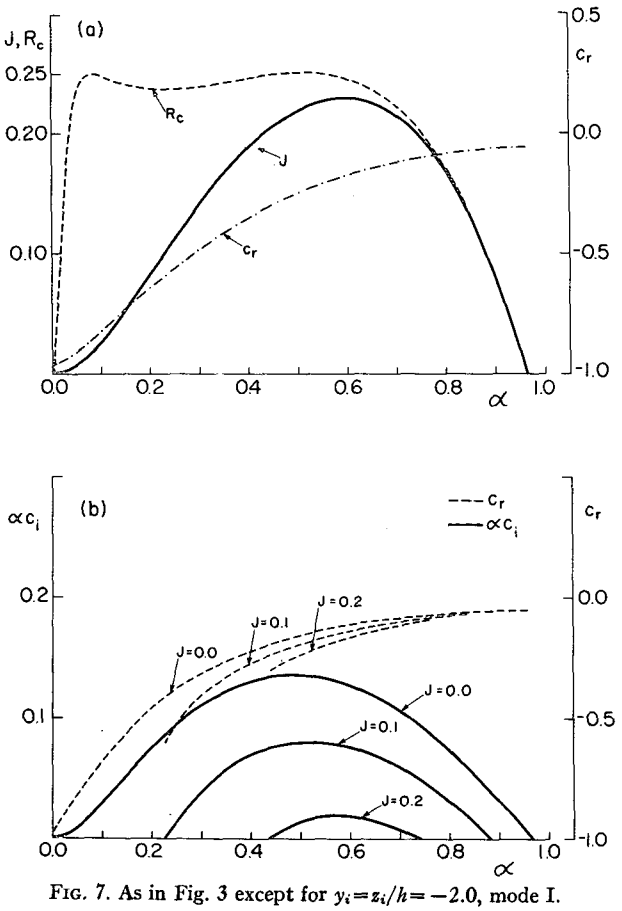

FIG. 7. As in Fig. 3 except for $y_i=z_i/h=-2.0$, mode I.

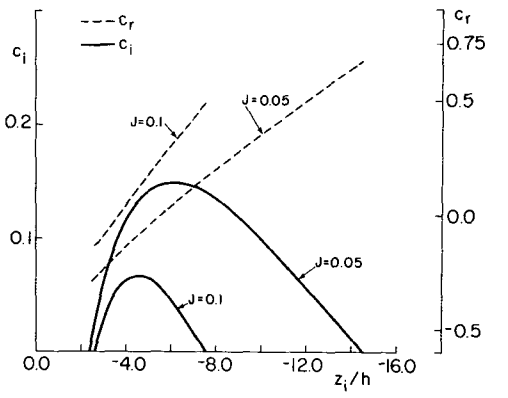

FIG. 8. Normalized imaginary c_i (solid line) and real c_r (dashed line) parts of the horizontal phase velocity of mode III unstable waves, for two different values of J, as a function of the normalized distance y_i between the inflexion point and the ground. Here $y_f=10.0$, $\alpha=0.01$ and $\sigma=0.1$.

To check the range of applicability of the above results, the validity of the Boussinesq approximation and the influence of the inertia terms, we have carried out extensive calculations with the fully compressible equations, as well as with $\sigma=0.0$ in Eq. (10). The results were substantially the same with the most noticeable difference in the values for c_r. This change in c_r does not affect the neutral boundary of mode I at all and results in a small shift upward, for mode II, of no more than 5%, and a shift downward, for mode III, of approximately 25% in the most extreme cases and of much less elsewhere. In future calculations, it is recommended that the fully compressible equations, as given for example by Chimonas (1970), be used since they do not introduce any new numerical problems. Thus approximations which are adequate for the present profiles need not be invoked.

TABLE 1. The approximate values of α and J at which αc_i is maximum of the entire αJ plane.

	$z_i/h=-10.0$		$z_i/h=-5.0$		$z_i/h=-2.0$	
	α	J	α	J	α	J
Mode I	0.46	0.0	0.46	0.0	0.48	0.0
Mode II	0.25	0.07	—		—	
Mode III	0.17	0.05	0.135	0.05	—	

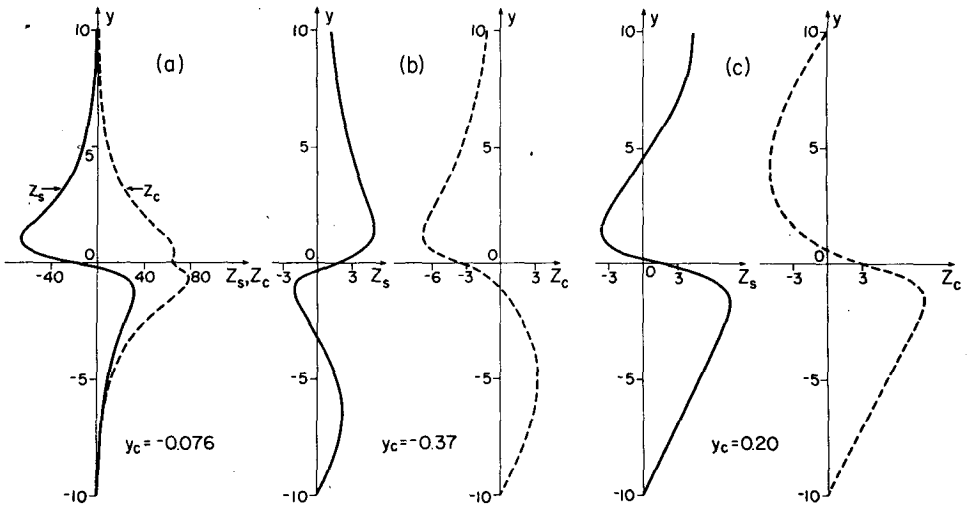

FIG. 9. Plots of $Z_c = \mathrm{Re}(\psi)$ and $Z_s = -\mathrm{Im}(\psi)$, the vertical velocities weighted by $\rho_0^{-\frac{1}{2}}$, for $J = 0.1$ and $\sigma = 0.1$: (a) mode I with $\alpha = 0.56$, $c_r = -0.07581$ and $c_i = 0.1974$; (b) mode II with $\alpha = 0.3$, $c_r = -0.3539$ and $c_i = 0.07298$; (c) mode III with $\alpha = 0.26$, $c_r = 0.1953$ and $c_i = 0.03475$. The wavelengths for each mode correspond to the most unstable wave for $J = 0.1$ as can be seen from Figs. 3 and 4.

For the results presented up to now, h is considered constant and therefore variations in $J = n^2h^2/V^2$ are due to variations in n^2/V^2. In Figs. 2–7 we choose $\sigma = h/H = 0.1$ which implies that H and n^2 are also constant, and thus variations in J are due entirely to variations in V. Yet since the presence of σ is found to have a small effect on the results as discussed above, within reasonable accuracy, variations in J can also be attributed to variations in n^2. In this approximation, the results can be applied to boundary layer situations as well. In either case, one cannot compare these results with the limiting case of the discontinuous Helmholtz profile studied by Lalas *et al.* (1976) for which $h \to 0$, but z_i and k_x remain finite.

b. Results for z_i constant and varying h

To study the effect of varying h, the equations are renormalized with respect to a length L, which we take to be proportional to z_i, a constant. The minimum

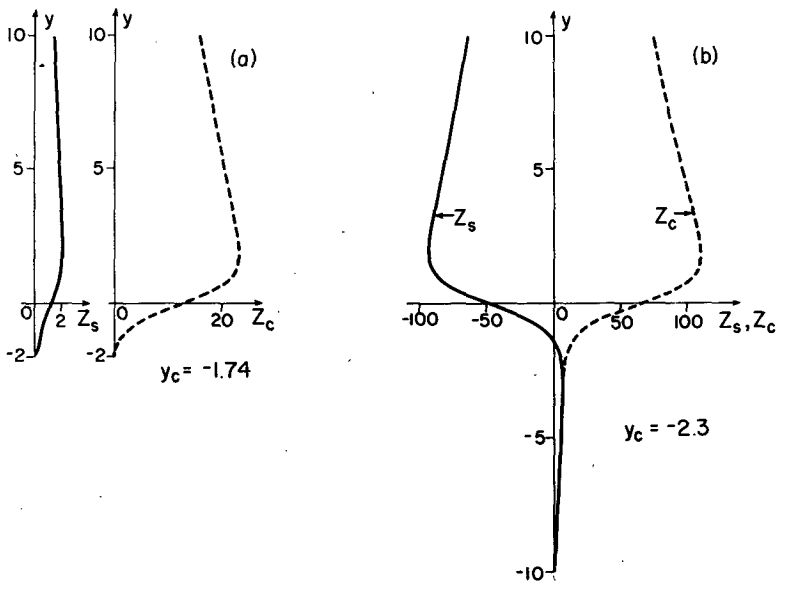

FIG. 10. Plots of Z_c and Z_s, the vertical velocities weighted by $\rho_0^{-\frac{1}{2}}$, for an unstable wave of mode I with $J = 0.0$, $\alpha = 0.01$ and $\sigma = 0.1$ to illustrate the effect of a change in y_i. (a) $y_i = z_i/h = -2.0$ for which $c_r = -0.9399$ and $c_i = 0.01969$; (b) $y_i = z_i/h = -10.0$ for which $c_r = -0.9802$ and $c_i = 0.08801$.

Richardson number J now becomes

$$J=\left(\frac{n^2L^2}{V^2}\right)\left(\frac{h^2}{L^2}\right)=\tilde{J}\left(\frac{h}{L}\right)^2, \tag{17}$$

and its variation is now due to changes of the ratio h/L, if we keep $\tilde{J}$ constant. For the following calculations, we choose $L=|z_i|/10$ and $\tilde{J}=0.0748$. These values of L and $\tilde{J}$ make the eigenvalues equal to the ones of the constant h case with $y_i=-10.0$, at $\alpha=0.01$ and $h/L=1.0$, which implies $J=0.0748$. The singular neutral mode plots in the $(\tilde{\alpha},J)$ plane, with $\tilde{\alpha}=k_xL=\alpha(L/h)$, are shown in Fig. 11. The limit $\tilde{\alpha}\to 0$ corresponds to $k_x\to 0$, and the limit $J\to 0$ corresponds to the Kelvin–Helmholtz discontinuous profile. The values of $\tilde{\alpha}$ for which the neutral curves cut the $J=0$ axis are $\tilde{\alpha}_{\rm Ia}=\tilde{\alpha}_{\rm Ib}\approx 0.25$, $\tilde{\alpha}_{\rm II}\approx 0.185$ with $c_{r\rm Ia}\approx -0.081$, $c_{r\rm Ib}\approx 0.0$ and $c_{r\rm II}\approx -0.46$; the renormalized vertical wavenumber K at large y is now approximately zero for all three modes although the zero is approached through imaginary values for modes Ia and II and real values for mode Ib. These values are in complete agreement with the results of Lalas *et al.* (1976) and can be calculated from their Eq. (31), with the appropriate translation of variables and normalizing quantities. In future numerical work, Eq. (31) of Lalas *et al.* (1976) can be used to provide initial starting points for all modes at $J=0.0$.

It should be pointed out that for $J=0.0$, we now have at least two modes, as opposed to the case with h constant, in which $J=0.0$ corresponds to zero stratification, and then only one, the Rayleigh (1880), mode is present.

Mode Ia,b is equivalent to the neutral mode calculated by Jones in his second model and shown in his Figs. 5 and 6. Mode II and the additional smaller modes not plotted here were not found by Jones.

The phase velocity of mode Ia varies between -0.08 at $\tilde{\alpha}=0.253$ to a minimum of -0.104 at $\tilde{\alpha}=0.37$ and goes toward -0.05 for large $\tilde{\alpha}$. Mode Ia is evanescent near the ground and at large heights. Mode II is also evanescent at large heights but propagating near the ground with $-1.0<c_r<-0.46$, while mode Ib is propagating on top and evanescent near the ground with c_r varying between 0.6 down to -0.03 as $\tilde{\alpha}$ increases. The neutral curves for modes Ia and II appear to asymptotically approach zero as $\tilde{\alpha}$ increases. The numerical calculation is stopped at the points shown in Fig. 11 only for the purpose of reducing computing time.

TABLE 2. Values of λ_z and δ_z as a function of Δy.

	Modes I ($\Delta y=9.92$)	II ($\Delta y=9.65$)	III ($\Delta y=10.19$)
$\delta_z/\Delta y$ above	0.206	0.527	4.28
$\lambda_z/\Delta y$ above	20.8	43.8	2.13
$\delta_z/\Delta y$ below	0.217	1.48	2.10
$\lambda_z/\Delta y$ below	12.8	1.72	14.17

c. *The effect of an abrupt increase of the static stability at large heights*

The static stability of the atmosphere is often observed to increase substantially at tropopause heights—a fourfold increase in n^2 is not unusual. Such an abrupt change in n^2 has been found in other studies, as, for example, in lee wave dynamics (Klemp and Lilly, 1975), to give rise to constructive interaction between upgoing and downgoing waves. To examine this effect, we modify the background Brunt–Väisälä frequency so that n^2 above $y=y_f$ is four times the value below. The neutral mode curve in the (α,J) plane is shown for h fixed, $y_i=-10.0$, $y_f=10.0$ and $\sigma=0.0$ in Fig. 12. The main feature is that the distinct structure of each

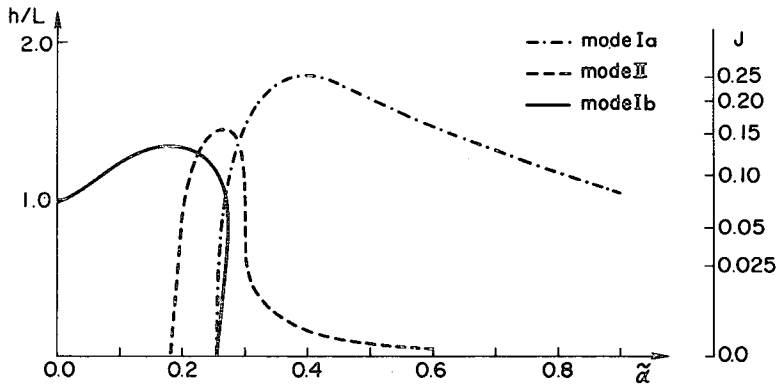

FIG. 11. Neutral wave plots in the $(\tilde{\alpha},J)$ or $(\tilde{\alpha},h/L)$ plane $[J=0.0748(h/L)^2]$ for the case of a variable thickness shear layer with the distance between the inflexion point and the ground equal to $10L$. The variation of density in the inertial term of the momentum equation is included. Note that $\tilde{\alpha}=k_xL=\alpha L/h$. Mode I comprises two branches, Ia evanescent and Ib propagating in the top layer.

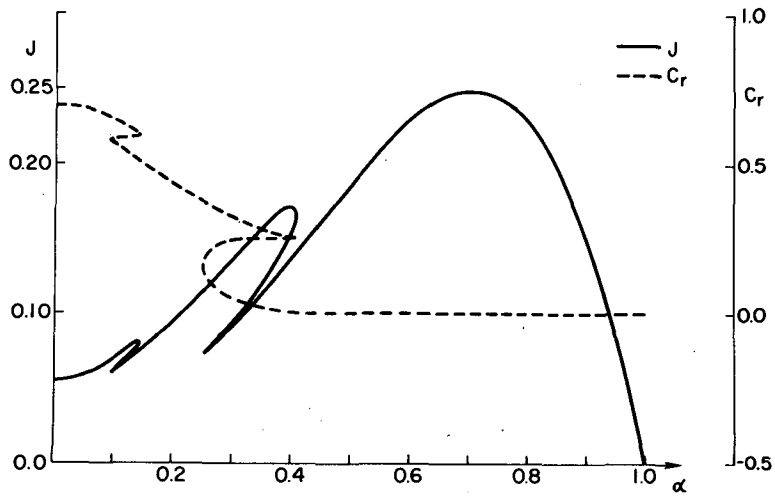

FIG. 12. Neutral wave plots in the (α,J) plane for $y_i=-10.0$, $y_f=10.0$ and $\sigma=0.0$ with n^2, the square of the Brunt–Väisälä frequency, above $y_f=10.0$ equal to four times n^2 below $y_f=10.0$.

mode has now disappeared. Vestiges of the modal structure remain, but now there are no separate neutral boundaries for each mode in the (α,J) plane projection. The neutral waves are propagating in the top layer $y>y_f$ and so are the unstable ones except for large values of α where they become mostly evanescent. The transition, though, in this case is continuous, with K_r/K_i going through 1 smoothly as α increases. No specific resonance was noticed in this particular example; the growth rates do not differ substantially for the case without a jump in static stability and the changes in the total unstable region in the (α,J) plane are small.

5. Conclusions

We have shown in this paper that an atmospheric shear layer, modeled by a hyperbolic-tangent velocity profile and a constant background temperature, in the presence of the ground, can support a number of unstable modes, in addition to the classical one discussed in the literature and labeled I in our figures. The properties of these modes and the consequences of their existence can be summarized as follows:

1) For given J and for each mode there exists a most unstable wave with wavelength λ_m. The values of λ_m for the additional modes are much larger than λ_m for mode I.

2) Unstable waves exist, for non-zero J, in the limit of $k_x \to 0$ and are always propagating in the top region. In the region near the ground they are either mostly propagating or mostly evanescent dependent on the actual value of J.

3) For a shear layer of given thickness, small wavelengths correspond to evanescent waves both above and below the shear layer. For large wavelengths there exist modes that are mainly propagating both above and below, or only above, or only below the layer. Such waves always belong to the additional modes, while mode I is always evanescent above and below the shear layer. The consequences of the ability of these waves to propagate and thus transport energy away from the shear layer are bound to be important in determining the vertical structure of the atmosphere and the coupling of mesoscale motions to microscale phenomena.

4) The growth rates of the additional modes are usually smaller than the corresponding ones for mode I and for the same J. As pointed out by Jones (1968), this is probably due to the fact that the propagation of energy away from the shear zone by the waves reduces the amount of energy available to them for temporal growth.

5) The system has the capability of exciting more than a single wavelength with maximum growth rate. This capability seems to be due to the presence of the ground which allows the kinematic conditions at the interface to be satisfied by more than one frequency and phase velocity by introducing an up-going wave in the layer between the shear zone and the ground. The ultimate wavelengths which will be observed in such a shear flow in the atmosphere will depend on a number of factors such as topography, horizontal inhomogeneities, initial growth rates as predicted by linear theory, as well as nonlinear effects. The latter have been studied recently by Tanaka (1975) who indicates that, for the only mode he has, long wavelength waves which have linear growth rates much smaller for given J than the short wavelength ones, may attain larger asymptotic amplitudes and may eventually become dominant.

Finally it should be mentioned that the possibility of

additional modes existing especially in the region of small values of α and large values of J cannot be excluded.

Characteristics of wave generation in actual atmospheric flows, once the velocity and temperature profiles are known, can be readily obtained by the present numerical technique, although care should be taken to insure that all modes of interest have been identified.

Acknowledgments. This research was supported in part by the Atmospheric Sciences Section, National Science Foundation, under Grants GA-32604 and DES 75-18866. We are grateful to the National Center for Atmospheric Research for providing the computer resources and facilities used for parts of these numerical calculations. Finally we would like to acknowledge many helpful discussions with Drs. D. K. Lilly and J. B. Klemp on several aspects of this work.

REFERENCES

Atlas, D., J. I. Metcalf, J. H. Richter and E. E. Gossard, 1970: The birth of "CAT" and microscale turbulence. *J. Atmos. Sci.*, **27**, 903–913.

Blumen, W., P. G. Drazin and D. F. Billings, 1975: Shear layer instability of an inviscid compressible fluid. Part 2. *J. Fluid Mech.*, **71**, 305–316.

Bulrisch, R., and J. Stoer, 1966: Numerical treatment of ordinary differential equations by extrapolation methods. *Num. Math.*, **8**, 1–13.

Chimonas, G., 1970: The extension of the Miles–Howard theorem to compressible flows. *J. Fluid Mech.*, **43**, 833–836.

Dickinson, R. E., 1973: Baroclinic instability of an unbounded zonal shear flow in a compressible atmosphere. *J. Atmos. Sci.*, **30**, 1520–1527.

——, and F. J. Clare, 1973: Numerical study of the unstable modes of a hyperbolic-tangent barotropic shear flow. *J. Atmos. Sci.*, **30**, 1035–1049.

Drazin, P. G., 1958: The stability of a shear layer in an unbounded heterogeneous inviscid fluid. *J. Fluid Mech.*, **4**, 214–224.

——, and L. N. Howard, 1966: Hydrodynamic stability of parallel flow of inviscid fluids. *Advances in Applied Mechanics*, Vol. 9, Academic Press, 1–89.

Einaudi, F., and D. P. Lalas, 1974: Some new properties of Kelvin–Helmholtz waves in an atmosphere with and without condensation effects. *J. Atmos. Sci.*, **31**, 1995–2007.

——, and ——, 1976: The effect of boundaries on the stability of inviscid stratified shear flows. *J. Appl. Mech.* (in press).

Emmanuel, C. B., 1973: Richardson number profiles through shear instability wave regions observed in the lower planetary boundary layer. *Boundary-Layer Meteor.*, **5**, 19–27.

Goldstein, S., 1931: On the stability of superposed streams of fluids of different densities. *Proc. Roy. Soc. London*, **A132**, 524–547.

Gossard, E. E., 1974: Dynamic stability of an isentropic shear layer in a statically stable medium. *J. Atmos. Sci.*, **31**, 483–492.

Hazel, P., 1972: Numerical studies of the stability of inviscid stratified shear flows. *J. Fluid Mech.*, **51**, 39–62.

Hines, C. O., 1974: *The Upper Atmosphere in Motion. Geophys. Monogr.*, No. 18, Amer. Geophys. Union, 248–328.

Hooke, W. H., F. F. Hall and E. E. Gossard, 1973: Observed generation of an atmospheric gravity wave by shear instability in the mean flow of the planetary boundary layer. *Boundary Layer Meteor.*, **5**, 29–41.

——, and K. R. Hardy, 1975: Further study of the atmospheric gravity waves over the eastern seaboard on 18 March 1969. *J. Appl. Meteor.*, **14**, 31–38.

Howard, L. N., 1961: Note on a paper by John W. Miles. *J. Fluid Mech.*, **10**, 509–512.

——, 1964: The number of unstable modes in hydrodynamic stability problems. *J. Mec.*, **3**, 433–443.

——, and S. A. Maslowe, 1973: Stability of stratified shear flows. *Boundary Layer Meteor.*, **4**, 511–523.

Hull, T. E., W. H. Enright, B. M. Fellen and A. E. Sedgwick, 1972: Comparing numerical methods for ordinary differential equations. *SIAM J. Num. Anal.*, **9**, 603–637.

Ince, E. L., 1956: *Ordinary Differential Equations*. Dover, 405 pp.

Jones, W. L., 1968: Reflexion and stability of waves in stably stratified fluids with shear flow: A numerical study. *J. Fluid Mech.*, **34**, 609–624.

Klemp, J., and D. K. Lilly, 1975: The dynamics of wave-induced downslope winds. *J. Atmos. Sci.*, **32**, 320–339.

Lalas, D. P., F. Einaudi and D. Fua, 1976: The destabilizing effect of the ground on Kelvin–Helmholtz waves in the atmosphere. *J. Atmos. Sci.*, **33**, 59–69.

Lindzen, R. S., 1974: Stability of a Helmholtz velocity profile in a continuously stratified, infinite Boussinesq fluid. Applications to clear air turbulence. *J. Atmos. Sci.*, **31**, 1507–1514.

——, and A. J. Rosenthal, 1976: On the instability of Helmholtz velocity profiles in stably stratified fluids when a lower boundary is present. Submitted to J. Geophys. Res.

Maslowe, S. A., and R. E. Kelly, 1971: Inviscid instability of an unbounded heterogeneous shear layer. *J. Fluid Mech.*, **48**, 405–415.

Miles, J. W., 1961: On the stability of heterogeneous shear flow. *J. Fluid Mech.*, **10**, 496–508.

——, and L. N. Howard, 1964: Note on a heterogeneous shear flow. *J. Fluid Mech.*, **20**, 331–336.

Rayleigh, Lord, 1880: On the stability, or instability, of certain fluid motions. *Proc. London Math. Soc.*, **11**, 57–70.

Reed, R. J., and K. R. Hardy, 1972: A case study of persistent, intense, clear air turbulence in an upper level frontal zone. *J. Appl. Meteor.*, **11**, 541–549.

Tanaka, H., 1975: Quasi-linear and non-linear interactions of finite amplitude perturbations in a stably stratified fluid with hyperbolic tangent-shear. *J. Meteor. Soc., Japan*, **53**, 1–31.

Taylor, G. I., 1931: Effect of variation in density on the stability of superposed streams of fluid. *Proc. Roy. Soc. London*, **A132**, 499–523.

Thorpe, S. A., 1969: Experiments on the stability of stratified shear flows. *Radio Sci.*, **4**, 1327–1331.

——, 1973: Turbulence in stratified fluids: A review of laboratory experiments. *Boundary Layer Meteor.*, **5**, 95–119.

Uccellini, L. W., 1975: A case study of apparent gravity wave initiation of severe convective storms. *Mon. Wea. Rev.*, **103**, 497–513.

Woods, J. D., 1968: Wave induced shear instability in the summer thermocline. *J. Fluid Mech.*, **32**, 791–800.